Available online at www.sciencedirect.com
ScienceDirect
International Journal of Mass Spectrometry 270 (2008) 156–165
International Journal of Mass Spectrometry
www.elsevier.com/locate/ijms

Effects of carbon dioxide in breath gas on proton transfer reaction-mass spectrometry (PTR-MS) measurements

L. Keck *, C. Hoeschen, U. Oeh

Institute of Radiation Protection, Helmholtz Zentrum München, German Research Center for Environmental Health (GmbH), Ingolstädter Landstr. 1, D-85758 Neuherberg, Germany

Received 23 November 2007; received in revised form 7 December 2007; accepted 10 December 2007
Available online 23 December 2007

Abstract

PTR-MS is becoming a common method for the analysis of volatile organic compounds (VOCs) in human breath. Breath gas contains substantial and, particularly for bag samples, highly variable concentrations of water vapour (up to ∼6.3%) and carbon dioxide (up to ∼6.5%). The goal of this study was to investigate the effects of carbon dioxide on PTR-MS measurements; such effects can be expected in view of the already well known effects of water vapour. Carbon dioxide caused an increase of the pressure in the PTR-MS drift tube (∼1% increase for 5% CO_2), and this effect was used to assess the CO_2 concentration of breath gas samples along the way with the analysis of VOCs. Carbon dioxide enhanced the concentration ratio of protonated water clusters ($H_3O^+H_2O$) to protonated water (H_3O^+) in the drift tube. Using the observed increase, being ∼60% for 5% CO_2, it is estimated that the mobility of water cluster ions in pure CO_2 is almost 65% lower than in air. Carbon dioxide had a significant effect on the mass spectra of the main breath gas components methanol, ethanol, 1-propanol, 2-propanol, acetone, and isoprene. Carbon dioxide caused a small increase (<10% for 5% CO_2) of the normalised main signals for the non-fragmenting molecules methanol and acetone. The increase can be much higher for the fragmenting VOCs (ethanol, propanol, and isoprene) and was, for 5% CO_2, up to ∼60% for ethanol. This effect of CO_2 on fragment patterns is mainly a consequence of the increased abundance of protonated water clusters, which undergo softer reactions with VOCs than the hydronium ions. Breath gas samples stored in Teflon bags lost ∼80% of CO_2 during 3 days, the decrease of VOC signals, however, is mainly attributed to decreasing VOC concentrations and to the loss of humidity from the bags.

Keywords: Breath gas analysis; PTR-MS; Carbon dioxide

1. Introduction

Proton transfer reaction-mass spectrometry (PTR-MS) is becoming a well established method to measure a number of volatile organic compounds (VOCs) in human breath gas [1–8]. Early studies demonstrated that the signals of several VOCs in PTR-MS mass spectra may feature variations by more than one order of magnitude; such variations can be interpreted reliably in terms of endogenous VOC concentrations, and the enhanced levels of acetonitrile for smokers are a common example [1–6]. Moreover, the PTR-MS features a fast response time, a good sensitivity, and samples can be analysed conveniently and quickly since no sample treatment is necessary. Hence, PTR-MS constitutes a promising technique for medical applications and particularly for the early diagnosis of common diseases, e.g., of lung cancer, with a non-invasive breath gas test [7,8]. Such a breath gas test, however, may demand the quantification of relatively small systematic differences in the VOC concentrations, and this poses a number of serious challenges. One problem is that the effect of the inhaled room air on the exhaled breath gas must be considered [9]. A second issue is the difficulty of collecting well defined breath gas samples [10], and such well defined breath gas samples are required not only for reproducible concentrations of VOCs, but also for reproducible concentrations of the bulk components.

For a normal resting person, the bulk composition of alveolar air features a mean volume mixing ratio of 74.9% nitrogen, 13.7% oxygen, 6.2% water vapour, and 5.3% carbon dioxide [11]. This bulk composition of alveolar air, however, depends on the sampling protocol, and for CO_2 it has been demonstrated

* Corresponding author. Tel.: +49 8931872943; fax: +49 8931872517.
E-mail address: keck@helmholtz-muenchen.de (L. Keck).

1387-3806/$ – see front matter © 2007 Elsevier B.V. All rights reserved.
doi:10.1016/j.ijms.2007.12.009

that the end-tidal concentration can be as low as 3.2% for high tidal volumes [12] and as high as 6.5% after breath holding [13]. Sample of mixed expired breath may feature even larger variations due to the contained portion air from the anatomic dead space because the CO_2 concentrations in the air from the dead space are much lower than the CO_2 concentrations in alveolar air. Moreover, breath gas is frequently sampled and stored in bags, and it will be shown below that such bags may loose not only the water vapour [14] but also almost completely the CO_2. Hence, breath gas samples contain not only a highly variable concentration of water vapour, but also a highly variable concentration of CO_2.

This variable bulk composition of the sample air is a major issue for PTR-MS analyses because, in contrast to the selected ion flow tube-mass spectrometry (SIFT-MS) technique where the buffer gas contains more than 95% of helium [15], the buffer gas in the drift tube of a PTR-MS is composed of the sample air. For water vapour, it is already well known that it has significant effects on the measured signals [16–18]. These effects are caused by the formation of protonated water dimers in the drift tube, which feature a lower mobility than protonated water and which react with the VOCs both via proton transfer and ligand switching reactions.

The aim of this study was to investigate whether the second additional component in breath gas, carbon dioxide, has similar effects on the measured signals. Unlike water vapour, CO_2 is not involved in the reactions in the drift tube. The mobility of small inorganic ions in CO_2, however, is much lower than their mobility in air, nitrogen, or oxygen; to give an example, the mobility of NO^+ in CO_2 at an E/N of 100 Td (1 Td = 1 Townsend = 10^{-17} V cm^2) is less than half of the mobility in air [19]. If similar differences occur for primary ions or VOCs, even CO_2 concentrations of a few percent could significantly change the reaction time in the drift tube. Due to the lower collisional energy, also changes of reaction rate constants, the formation of clusters, and fragmentation patterns may occur, with so far unknown effects on the measured signals.

These effects of CO_2 on PTR-MS signals must be considered for a proper calibration of the instrument for breath gas analysis, and they are essential for the desired comparison of room air and breath gas concentrations. Moreover, the early diagnosis of diseases could potentially require the evaluation of small systematic changes of breath gas VOC patterns; therefore, it must be guaranteed that apparent differences in PTR-MS mass spectra are not caused just by a different bulk composition of the samples. The effects of CO_2 should also be considered for a proper interpretation of exhalation profiles, and finally also for headspace analyses of cells, in which a gas mixture with 5% CO_2 is commonly used [20].

2. Experimental

All measurements were conducted with a commercial standard PTR-MS (Ionicon Analytic GmbH) as described by Lindinger et al. [21] and Hansel et al. [22]. The instrument, schematically shown in Fig. 1, consists of (i) the ion source to produce hydronium primary ions, (ii) the drift tube where the proton transfer reaction occurs, and (iii) a detection system with a quadrupole mass spectrometer (QMS) and a secondary ion multiplier (SEM).

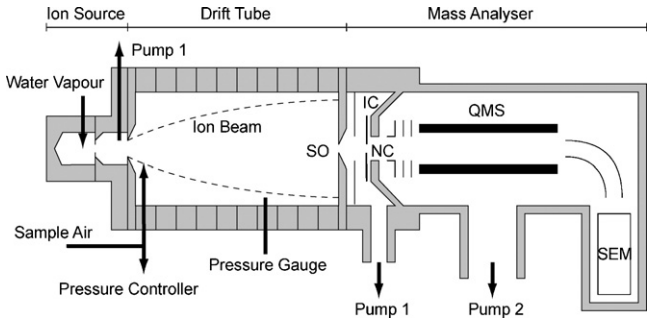

Fig. 1. Schematic diagram of the PTR-MS instrument. SO, sampling orifice; IC, intermediate chamber; NC, nosecone; QMS, quadrupole mass spectrometer; SEM, secondary electron multiplier.

The pressure in the drift tube P_d, typically ~2 mbar, was measured with a membrane-based pressure gauge (Pfeiffer CMR 263) with an accuracy of 1 μbar. A portion of the pressure in the drift tube, $P_{d,s}$, is caused by the ion source, and for our settings $P_{d,s}$ equals ~580 μbar. The portion of the pressure in the drift tube which is attributed to the sample is referred to as reduced pressure $P_{d,red}$ with $P_{d,red} = P_d - P_{d,s}$. The flow rate of sample air into the drift tube and hence the pressure in the drift tube is regulated with a pressure controller [16]; the pressure upstream of the controller is denoted as bypass pressure P_{by}. The pressure in the drift tube showed sometimes small periodic variations with a periodic time of several minutes; these variations originate probably from the regulation of the pressure controller. To eliminate these variations, P_d was always alternately measured for the analyte gas sample and for a sample of synthetic air within less than ~15 s, and the difference between the two values of P_d is referred to as ΔP_d.

An electric field E is applied parallel to the drift tube axis in order to reduce the formation of cluster ions. Commonly an E/N of 120–140 Td is chosen for the measurements, with N being the number density in the drift tube. For all VOCs, mass spectra from 20 to 200 amu were measured with a dwell time of 0.5 s. The raw count rates refer to the mean values from typically seven scans, and the measured counts per seconds on mass X are denoted as cps(X). The signal of the primary ions, cps(19), was calculated from the signal of the isotopoloque, cps(21). To account for the non-linear response of the SEM, an experimentally determined correction factor was used for high signals from water clusters, cps(37). This correction, being 15% at maximum, affects the results only slightly.

The samples were prepared from synthetic air, i.e., 20% O_2 and 80% N_2 ("SA-0%"), and from two custom-made gas mixtures, the first mixture consisting of nominally 5% CO_2, 15% O_2 and 80% N_2 (SA-5%) and the second mixture of 10% CO_2, 10% O_2 and 80% N_2 (SA-10%). The pressurised gas cylinders with these mixtures were prepared by Linde AG from pure gases in 5.0 purity (99.999%). Additionally, pure N_2, O_2, CO_2 and Argon were used in purity 4.5 (99.995%) or higher. The pressurised gases were filled in Teflon sample bags; the bags consist of

polytetrafluoroethylene (PTFE) Teflon membrane (Welch Fluorocarbon) with a PTFE valve of our own design ("PTFE bag"). Breath gas samples were collected in the PTFE bags or in ready-made commercial sample bags (SKS Inc.) with a fluorinated ethylene–propylene (FEP) Teflon membrane ("FEP bag").

Mixtures and dilutions were prepared by two methods: the first method ("syringe method") employed a 100 ml syringe made of borosilicate glass. The syringe was connected with three bags by valves; bags 1 and 2 contained the gases to be mixed and bag 3 the mixture. The desired volume of gas was extracted from bags 1 and 2 with the corresponding number of strokes of the syringe and pumped into bag 3. The second method ("flow meter method") employed a digital flow meter (Analyt-MTC GmbH). The flow meter was first used to measure the total flow into the PTR-MS, F_{tot}. When bags are used, the inlet is at atmospheric pressure and F_{tot} is constant. Then two bags, 1 and 2, were connected with a branch connection to the PTR-MS and the flow from bag 1, F_1, was measured with the flow meter. The mixing ratio of the two gases was adjusted with a switching valve at the branch connection, and it was calculated from F_{tot}, and F_1. Humidification of the bag samples was accomplished by spiking the bags with ultrapure deionised ("DI") water followed by evaporation in an oven for 15 min at 60 °C.

The samples of the main breath gas components, methanol, ethanol, 1-propanol, 2-propanol, acetone and isoprene, were based on liquid solutions, all liquids had a purity >99%. In a first step, concentrated samples were prepared by placing tiny droplets in a bag that was thereafter filled with SA-0%. To adjust a suitable concentration, the bag was connected to the PTR-MS and the decrease of the primary signal was observed. The sample was diluted with SA-0% until a decrease of the primary signal by ∼30% was achieved. In a second step, 100 ml of these concentrated samples were mixed, using the syringe method, with 1400 ml of SA-0%, SA-5% and SA-10% and the resultant 6.7% relative decrease of CO_2 concentrations was considered for the data evaluation.

3. Results and discussion

It was found that the CO_2 concentration of breath gas samples can be conveniently assessed from the pressure in the drift tube. It is pointed out that CO_2 causes an increase of water cluster concentration in the drift tube and that this increased water cluster concentration has a significant effect on the fragmentation pattern of breath gas VOCs. This finding constitutes our main result. Finally, it is demonstrated that bag samples can lose CO_2 almost completely.

3.1. Pressure in the drift tube

An obvious effect during breath gas analyses is the increase of the drift tube pressure P_d when breath gas enters the PTR-MS, and we suspected that the increase of P_d is caused by the modified composition of the buffer gas. To verify this suspicion, ΔP_d was measured for the main components of breath gas as listed in Table 1. In order to achieve large changes, pure gases were used for N_2, O_2, Ar, and CO_2. Synthetic air saturated with water vapour at 37 °C, i.e., 6.3% of water vapour in synthetic air, was used for water vapour. This water vapour concentration corresponds to the concentration in alveolar breath and it is almost the highest concentration that can be measured because higher concentrations cause condensation in the inlet system and in the drift tube of the PTR-MS. The measurements were performed for a bypass pressure of 340 and 380 mbar and the values are denoted as $\Delta P_{d,340}$ and $\Delta P_{d,380}$, respectively. For synthetic air, these P_{by} correspond to a P_d of ∼1885 and ∼2176 μbar, and to a $P_{d,red}$ of 1305 and ∼1596 μbar, respectively.

Table 1
Change of pressure in the drift tube with respect to synthetic air, measured for a bypass pressure of 340 and 380 mbar and denoted as $\Delta P_{d,340}$ and $\Delta P_{d,380}$

Sample	$\Delta P_{d,340}$ (μbar)	$\Delta P_{d,380}$ (μbar)	$\Delta P_{d,380}/\Delta P_{d,340}$	c_i (10^{-2})
N_2 (pure)	+17	+22	1.29 ± 0.14	+1.18 ± 0.1[a]
O_2 (pure)	−61	−71	1.16 ± 0.04	−4.73 ± 0.1[a]
Ar (pure)	−37	−45	1.21 ± 0.06	−2.89 ± 0.1
CO_2 (pure)	+478	+580	1.21 ± 0.01	+36.74 ± 0.1
H_2O (6.3%)	−1[b]	−1.5[b]	1.5 ± 1	−1.48 ± 1

The coefficients in the last column can be used to calculate ΔP_d for arbitrary compositions of the sample gas using Eq. (1).
[a] Values adjusted for consistency with $\Delta P_d = 0$ μbar for SA-0%.
[b] Mean values from 3 experiments.

The results, listed in Table 1, indicate that each gas has an effect on P_d, but that CO_2 causes by far the strongest increase. Moreover, the ratio $\Delta P_{d,380}/\Delta P_{d,340}$ is constant and equal to the ratio of $P_{d,red}$ at a bypass pressure of 380 and 340 mbar, 1.22. Hence, it was assumed that ΔP_d is proportional to $P_{d,red}$. In addition, measurements of synthetic air and CO_2 in variable mixing ratios showed a nearly linear relation between fractional gas concentration and ΔP_d. These results suggest that the change of pressure in the drift tube can be approximated by the formula

$$\Delta P_d = P_{d,red} \sum_i c_i f_i \quad (1)$$

where f_i is the fractional concentration of the gas i and c_i the dimensionless gas specific coefficient listed in Table 1.

More detailed investigations on the causes of this effect are beyond the scope of this work. We assume, however, that P_d is mainly controlled by the molar mass or the dynamic viscosity of the gas, with P_d increasing for high molar mass and low dynamic viscosity. This idea is prompted by additional tests where Xenon, featuring particularly low dynamic viscosity and high molar mass, caused an excessive increase of P_d. In addition, we suspect that the reported values are also affected by the type of turbomolecular pump (shown as pump 1 in Fig. 1) and by geometric details of the gas inlet and outlet.

Eq. (1) can be used to calculate ΔP_d for the custom-made gas mixture and there was a perfect agreement between measured and calculated values for SA-10%. For SA-5%, the measured values of ΔP_d are consistent with a composition of 80% N_2, 16% O_2, and 4% CO_2; these values are within the accuracy specified by the manufacturer and they were adopted for the data evaluation.

For breath gas samples, an increase of the CO_2 concentrations in breath gas is accompanied by an equal decrease of the oxygen concentrations. Moreover, it is assumed that nitrogen, argon, oxygen, and CO_2 are diluted by water vapour at saturation vapour pressure. With these assumptions, Eq. (1) can be used to calculate the carbon dioxide concentrations of the sample in %, $c(CO_2)$, from

$$\Delta p_d = -a + b \cdot c(CO_2) \quad (2)$$

with $a = -2$ and -3 μbar and $b = 5.4$ and 6.6 μbar for a bypass pressure of 340 and 380 mbar, respectively. These CO_2 concentrations, assessed along the way with PTR-MS measurements, constitute valuable information. For fresh breath gas samples and normal breathing, the CO_2 concentration reflects the portion of alveolar air. Hence, CO_2 concentration can be used to normalise VOC-concentrations with respect to the portion of alveolar air [23], or to identify samples, which, due to occasional incorrect sampling, contain a low portion of alveolar air and which must be excluded from further analysis. Moreover, the usual decrease of breath gas CO_2 concentrations during heavy exercise can be assessed [3,12]. Finally, the CO_2 concentrations can also be used to estimate the ageing effect of bag samples, which may lose CO_2 completely (see Section 3.4).

3.2. Water cluster ions

Water cluster ions in the drift tube of the PTR-MS occur mainly as $H_2O{\cdot}H_3O^+$ and are detected as cps(37). They originate partly from water vapour of the ion source [16], but the concentrations increase strongly with increasing humidity of the sample air [24]. To investigate the effect of CO_2 on the concentration of water cluster ions, dry and wetted mixtures of SA-0% and CO_2 were measured. The mixing was carried out with the flow meter method and the signals of cps(19) and cps(37) were monitored. The results, shown in Fig. 2, indicate the expected increase of water cluster concentration at higher humidity. The data points for $CO_2 = 0\%$ show similarity to the measurements of Ammann et al. [24], who found a quadratic relation of humidity and water cluster concentrations. In addition, however, there is a steep and nearly exponential increase of the water cluster concentrations with increasing CO_2 concentration. For a humidity of 4.7% an increase of the CO_2 concentration by 5% leads to an increase the water cluster concentration by 54% for $P_{by} = 340$ mbar and by 67% for $P_{by} = 380$ mbar. Hence, the signals of water cluster ions are by no means controlled only by the humidity of the sample [14,25], but they are substantially affected also by the CO_2 concentration.

Following de Gouw et al. [16], the ratio of $[H_2O{\cdot}H_3O^+]/[H_3O^+]$ in the drift tube is controlled by the kinetic energy in the center of mass system for the collision of water cluster ions and buffer gas molecules, KE_{cm}, and the ratio decreases with increasing KE_{cm}. As the buffer gas and reacting neutral molecules are identical, KE_{cm} is simply [16]

$$KE_{cm} = \tfrac{1}{2} m_b v_d^2 + \tfrac{3}{2} k_B T \quad (3)$$

with v_d being the drift velocity, k_B the Boltzman constant, T the temperature in K and m_b the mass of the buffer gas. The observed increase of water cluster concentration implies a decrease of KE_{cm} with increasing CO_2 concentrations. Since the molecular mass of CO_2 is much higher than that of air, the drift velocity of water cluster ions in CO_2 must be, according to Eq. (3), much lower than in air. The increase of the water cluster ions concentration shown in Fig. 2 can be used to estimate the drift velocity and mobility of water clusters in CO_2 as follows:

The observed ratio cps(37)/cps(19) can be decreased by collision-induced dissociation of water cluster ions in the intermediate chamber [16,18] between drift tube and nosecone of the QMS (see Fig. 1) or, as suggested by Steinbacher et al. [26], be enhanced by the jet that is formed at the outlet orifice of the drift tube. Nevertheless, with potentials optimised in order to minimise the collision-induced dissociation, de Gouw et al. [16] found a reasonable agreement between observed and calculated ratio cps(37)/cps(19) for $E/N > 95$ Td, corresponding to $KE_{cm} > 0.11$ eV. Similar to de Gouw et al. [16], cps(37)/cps(19) was measured for dry synthetic air as a function of KE_{cm} by varying the pressure in the drift tube. The results in Fig. 3 indi-

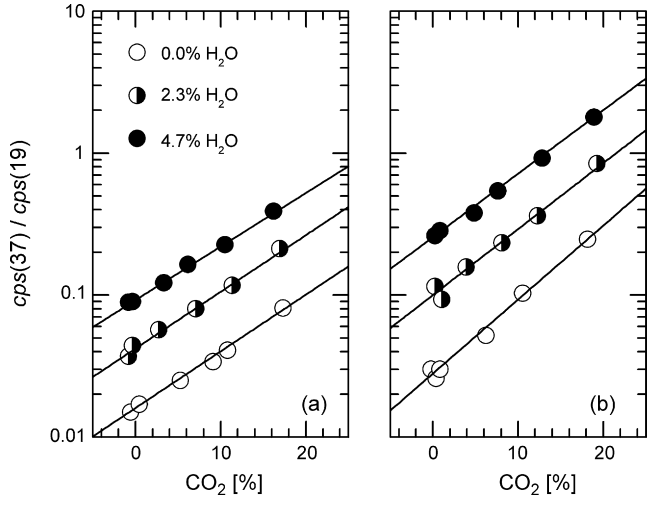

Fig. 2. Effect of CO_2 on water cluster concentrations. (a) Measured at 137 Td and (b) at 119 Td.

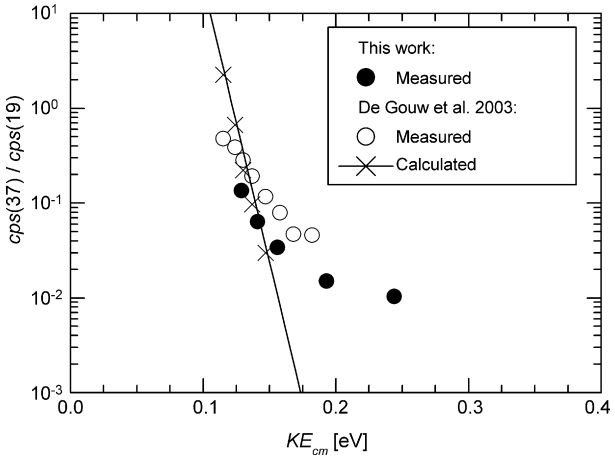

Fig. 3. Water cluster concentrations as a function of kinetic energy, KE_{cm}.

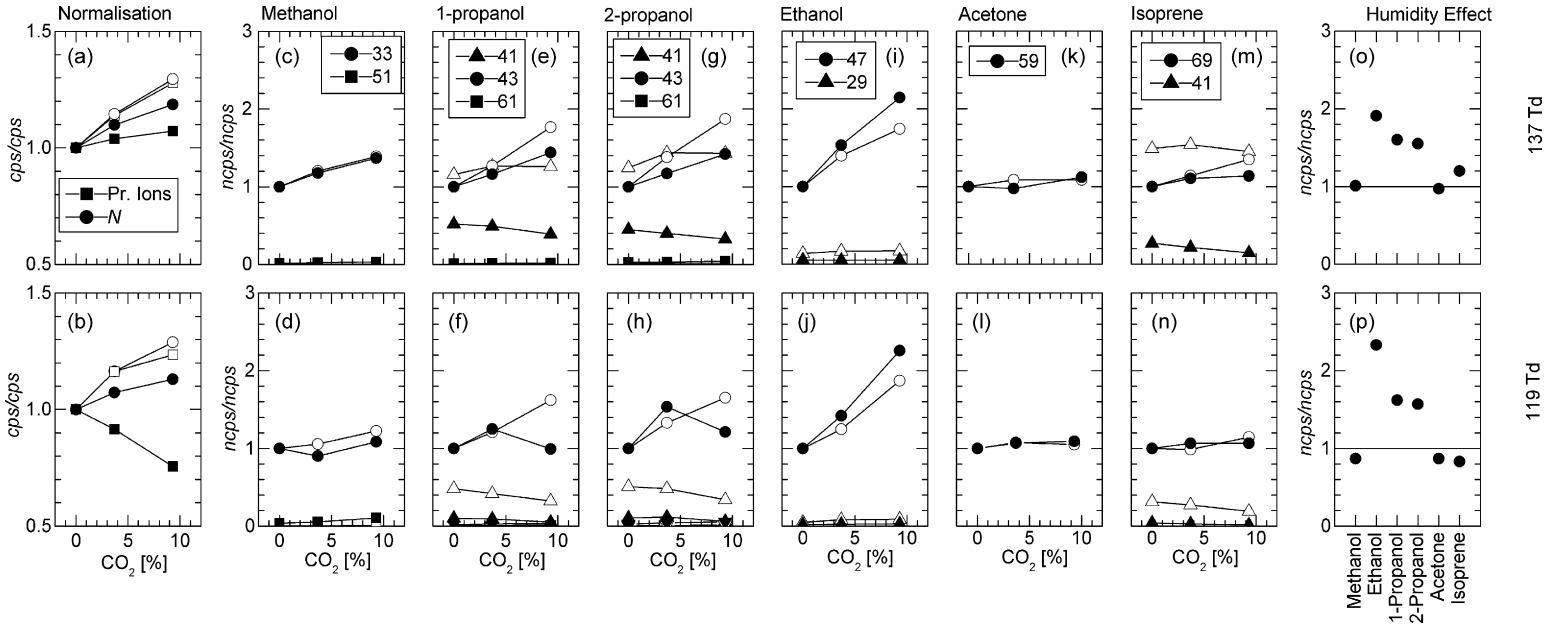

Fig. 4. Effect of CO_2 on the signals from primary ions, on the normalisation factor N, and on normalised signals ncps of breath gas VOCs. The upper panels refer to measurements at $E/N = 137$ Td, the lower panels to 119 Td. Open symbols: dry samples; solid symbols: samples with a humidity of 6.3%. All values are scaled with respect to the main signals at a CO_2 concentration of 0%.

cate that the ratio measured by us is lower, presumably because the potentials of the intermediate chamber were not optimised. The decrease of the log(cps(37)/cps(19)) with increasing KE_{cm} in the relevant range of 0.16–0.20 eV, however, is still similar to previous measurements and we assume that these variations of cps(37)/cps(19) are still mainly controlled by KE_{cm}.

Using Eq. (3), KE_{cm} was numerically calculated as a function of the fractional CO_2 concentration, with the mobility of water cluster ions in CO_2 as the only unknown parameter. For that the definition of the ion mobility μ

$$v_d = \mu E \tag{4}$$

with

$$\mu = \mu_0 \frac{T}{273\,\mathrm{K}} \frac{1013\,\mathrm{mbar}}{p_{drift}}, \tag{5}$$

was used; p_{drift} is the drift tube pressure in mbar, T the drift tube temperature in K, and μ_0 is the reduced mobility for the mixture of air and CO_2. Moreover, Blancs law

$$\frac{1}{\mu_0} = \frac{f_1}{\mu_{0,1}} + \frac{f_2}{\mu_{0,2}} \tag{6}$$

was used to calculate the reduced mobility of gas mixtures, where $\mu_{0,1}$ and $\mu_{0,2}$ are the reduced mobilities of water cluster ions in air and CO_2, and f_1 and f_2 the corresponding fractional gas concentrations. The reduced mobility of water cluster ions in air, 2.8 $cm^2\,V^{-1}\,s^{-1}$, was adopted from Warneke et al. [17]. The calculation also included the increase of p_{drift} and m_b with an increasing fractional CO_2 concentration f_2. The decrease of KE_{cm} with increasing f_2 can be expressed as

$$\frac{\partial KE_{cm}(\mu_{0,2})}{\partial f_2} = \frac{\partial\ \log(cps(37)/cps(19))}{\partial f_2} \times \left(\frac{\partial\ \log(cps(37)/cps(19))}{\partial KE_{cm}} \right)^{-1}, \tag{7}$$

with the first and second term on the right side being displayed in Figs. 2 and 3. Note that the decrease of cps(37)/cps(19) by the collisions in the intermediate chamber cancels out. Using Eq. (7) the reduced mobility of water cluster ions in CO_2, $\mu_{0,2}$, turns out to be ~1.0 $cm^2\,V^{-1}\,s^{-1}$, which is almost 65% lower than the mobility in air. The mobility in breath gas, i.e., a mixture of air with 5% CO_2, calculated from Blanc's law, is 8% lower than in air without CO_2. These values, however, should be considered just as a best guess mainly because of, the large error of the second term in Eq. (7), as obvious from Fig. 3.

3.3. VOC signals

Normalised count rates are used for the discussion of the VOC signals on mass X. These normalised count rates, ncps(X), are defined by

$$ncps(X) = cps(X)\frac{10^6\,s^{-1}}{N} = cps(X)\frac{10^6\,s^{-1}}{cps(19) + cps(37)}. \tag{8}$$

N denotes a normalisation factor which reflects the sum of primary ions and water cluster ions. This normalisation takes into account that methanol, ethanol, acetone, isoprene react with water cluster ions at a similar reaction rate constant as with the primary ions [15], and this was assumed also for propanol. These reactions with water clusters occur by ligand switching since all studied VOCs are polar; for acetone and isoprene, featuring a proton affinity (PA) higher than 8.40 eV, also by direct proton transfer reaction [27]. For the normalisation, recent environmental studies [28] additionally used a molecule-specific weighting factor for cps(37). This weighting factor contains reaction rate constants and transmission efficiency of the mass analyser, and it was experimentally determined. The weighting factor, however, could be determined neither for ethanol nor for propanol because probably not all fragments were detected. Hence, this weighting factor was omitted for the sake of consistency. Using the weighting factor, being less than unity, would not substantially change our results; it has a negligible effect for dry samples anyhow and would cause a somewhat stronger increase of the normalised signals with increasing CO_2 concentrations for the wet samples.

As shown in Fig. 4a and b, with the example of the measurements of methanol, there is an increase of the primary ions for the dry samples with increasing CO_2 concentrations. The increase of the primary ion signal is weaker for the humid samples, and at 119 Td there is even a decrease because most of the primary ions are consumed for the formation of water cluster ions. The normalisation factor N, however, shows an increase at higher CO_2 concentration both for 137 and 119 Td because of the increasing portion of the water cluster ions (Fig. 3). Consequently, the increase of VOC signals with increasing CO_2 concentration is much stronger if the normalisation is omitted or done with respect to the primary signal. Previous breath gas studies have not always clearly stated the way of normalisation [1–5,8], hence these results could be much more affected by CO_2 than the normalised signals of this study.

Monitoring the drift tube pressure indicated that the loss of CO_2 from the bags, described in Section 3.4, was less than 10%. However, to keep these losses low, only a few measurements were performed with a single filling. Therefore, CO_2 effects were measured first for a dry sample, then for a wet sample, and finally, with a third filling of the bag, the difference between wet and dry samples was measured for SA-0%. As equal concentrations for dry and humid samples cannot be expected, the ncps were scaled separately for dry and humid samples so that the main signals are equal to unity at 0% CO_2. Main signals refer to the masses which are commonly used to quantify the substances, 33 for methanol, 47 for ethanol, 43 for 1-propanol and 2-propanol, 59 for acetone and 69 for isoprene. These scaled data are presented in Fig. 4c–n; the humidity effect, i.e., the ratios of the main signals from wet and dry samples, is shown in Fig. 4o and p. The CO_2 effects are shown only for fragments or clusters with signals higher than 10% of the main signals, except for propanol where the signal of unfragmented molecules is shown for the sake of completeness. The combined error, originating from the dilution, the measurement of the signal, and the normalisation and scaling is estimated to be 10–15%.

The results for the tested VOCs were as follows: *Methanol* (Fig. 4c and d): The signal of the protonated methanol on mass 33

increased with increasing CO_2 concentrations for $E/N = 137$ Td. The increase is weaker for $E/N = 119$ Td, particularly for the humid samples. A small portion of methanol was detected as cluster ions on mass 51. *1-Propanol* (Fig. 4e and f) and *2-propanol* (Fig. 4g and h): The two isomers of propanol behaved quite similarly. The signal of protonated propanol, mass 61, was always less than 5% of the signal of the fragment detected on mass 43, $C_3H_7^+$ [29]. At 137 Td, both mass 43 and 61 showed a clear increase with increasing CO_2 concentrations, and the increase was more pronounced for dry samples. At 119 Td, wet samples displayed a maximum for mass 43. The height of this maximum, however, is somewhat uncertain because the signals of mass 43 for wet samples sometimes featured instabilities which do not occur for any other signal. High signals were also detected for mass 41, probably from $C_3H_7^+$. The signal on mass 41 decreased with increasing CO_2 concentrations for $E/N = 119$, for $E/N = 137$, however, the signal decreased for the humid samples whereas it increases for the dry samples. *Ethanol* (Fig. 4i and j): The signal of the protonated molecule, mass 47, was approximately two times higher at 10% CO_2 than at 0% CO_2 and featured the strongest increase with increasing CO_2 concentration among the tested substances. The signal of the fragment on mass 29, $C_2H_5^+$ [30], was lower for the wet samples and increased as well with increasing CO_2 concentrations. *Acetone* (Fig. 4k and l): There was no significant effect on the signal of protonated acetone, mass 59. *Isoprene* (Fig. 4m and n): There was a clear increase for the signal of protonated isoprene, mass 69 at $E/N = 137$ Td and a less pronounced increase at $E/N = 119$ Td. The signal of a fragment on mass 41, $C_3H_5^+$ [30], was higher for lower E/N and for dry samples. It decreased with increasing CO_2 concentrations, the decrease was however not significant for dry samples at $E/N = 137$ Td. These observed trends are caused by the combined effects of CO_2 on (i) drift tube pressure, (ii) ion mobility, (iii) reaction rate constants, (iv) water cluster concentrations, and (v) fragmentation pattern; and the effects will be addressed in this order:

(i) The increase of P_d, is ∼1% for 5% CO_2. Additional experiments showed that an increase of P_d by 1% at constant electric field corresponds to an increase of the ncps by 2–3%, similar to previous findings [16]. This is only a small contribution to the observed changes shown in Fig. 4.

(ii) The density of reaction products at the end of the drift tube $[RH^+]$ is [31]

$$[RH^+] = \frac{k \cdot L \cdot [R] \cdot [H_3O^+]}{\mu_{RH}} \quad (9)$$

with k the reaction rate constant, L the length of the drift tube, $[R]$ the concentration of VOCs, $[H_3O^+]$ the concentration of the primary ions and μ_{RH} the mobility of the reaction products. Let us assume that the CO_2 causes an equal decrease of the mobility by a factor a, equally for $[H_3O^+]$ and $[RH^+]$. If the flux of hydronium ions from the ion source is constant, this causes an increase of $[H_3O^+]$ by the factor a, and together with the decrease of μ_{RH}, an increase of $[RH^+]$ by a factor a^2. There are still doubts [31] whether the detected count rates are proportional to the concentration or to the flux. The decrease of the mobilities, however, would in any case result in an increase of the normalised count rates by a factor a. Hence, if 5% of CO_2 reduce, as for the water cluster ions, ion mobilities by 8%, an increase of the ncps by ∼8% can be expected. This value resembles the mean observed increase for the VOCs without significant fragmentation, methanol and acetone. Hence, it is supposed that such small increases are mainly caused by the reduced mobility.

(iii) Since all investigated molecules are polar, reaction rate constants vary because of the CO_2 induced change of KE_{cm} [32]. Published data for proton transfer reactions with methanol, ethanol, acetone [33], 1-propanol, 2-propanol [29] and isoprene [30] indicate that 5% of CO_2 would cause a decrease of the reaction rate constant by a few percent for these molecules, except for isoprene where the decrease is negligible. This constitutes only a minor contribution to the observed differences.

(iv) CO_2 concentration causes an increase of water clusters concentrations. Hence, a larger portion of the reaction products originates from the reactions with water clusters, but the effect on ncps should be low. Moreover, water cluster ions feature a lower mobility than hydronium ions, and the two species are in equilibrium between the formation and collision-induced dissociation [17]. Hence, a higher portion of water clusters implies a lower effective mobility of the reacting ions. Assuming a constant flux from the ion source, this causes a higher density of the reacting species at the end of the drift tube and, according to Eq. (9), also a higher density of reaction products. The effect on the ncps, however, cannot be predicted since it depends on the question whether the measured count rates are proportional to the density or to the flux of the ions [31]. The increasing portion of water clusters also boosts the formation of cluster ions with VOCs. The effect is significant for methanol where for wet samples at 119 Td a portion of methanol is consumed for the formation of the cluster ion on mass 51.

(v) A significant amount of fragments was detected for ethanol, propanol, and isoprene. Fig. 4 shows that the effects of CO_2 are stronger for ethanol and propanol than for isoprene. Moreover, for ethanol and dry samples of propanol at 137 Td, there is a strong increase of the main signals but no corresponding decrease of signals from fragments. From that it is concluded that not all fragments were detected for ethanol and propanol, and that the increase of their detected main signals occurs on the expense of undetected fragments. For ethanol, previous studies detected a fragment on mass 19, H_3O^+; the portion decreases strongly with increasing KE_{cm} [30] and presumably also with increasing ratio cps(37)/cps(19). This fragment is not detectable with our setup, but it was probably abundant, because the amount of ethanol evaporated in a bag, needed for a given decrease of the primary signal, was much larger than for all other substances. We speculate that the undetected fragments of propanol are also on mass 19, and that a low amount of such fragments may occur even for methanol. The strong effect of CO_2 on the fragmentation of ethanol and propanol is also

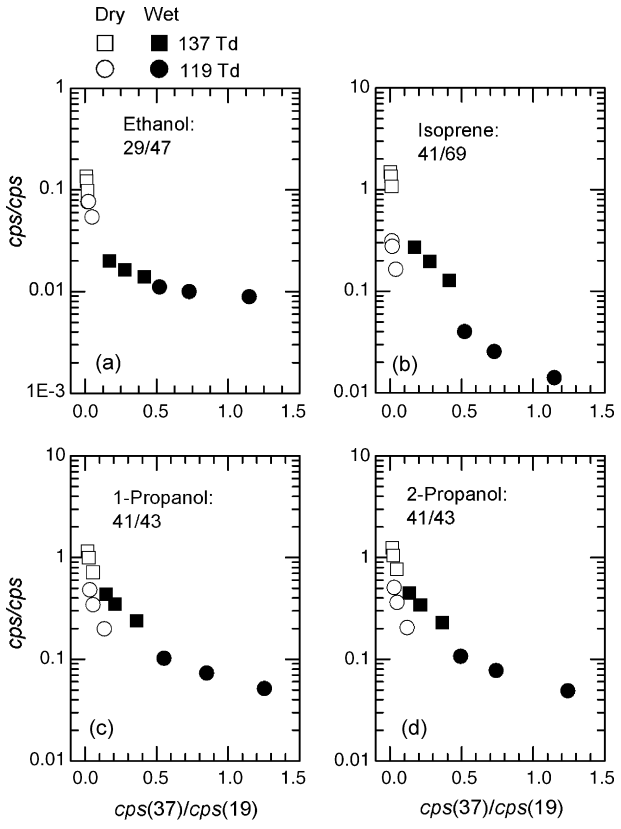

Fig. 5. Ratio of signals from VOC fragments as a function of the ratio cps(37)/cps(19).

echoed by the large humidity effects for the main signals, shown in Fig. 4o and p.

Fig. 5 shows the ratios of major fragments to main signal as a function of cps(37)/cps(19) for the fragmenting VOCs. For ethanol, Fig. 5a, the ratio is essentially completely determined by cps(37)/cps(19), and also for isoprene and propanol the main portion of the variation can be explained by the level of water cluster ions. Fig. 5 shows that there is as well a second and smaller effect of the fragmentation, namely the influence of KE_{cm} [29]. This effect is visible particularly for wet samples with 0% CO_2 at 137 Td, featuring a similar ratio cps(37)/cps(19) as dry samples with 10% CO_2 at 119 Td, but displaying a clearly higher ratio of signals. From that, it would be expected that there is basically also an effect of CO_2 on the fragmentation by its effect on KE_{cm}; this, however, seems to be a minor contribution as the decrease of the ratios in Fig. 5 with increasing CO_2 concentrations is hardly different from the overall decrease with increasing ratio cps(37)/cps(19). Hence, the effects of both CO_2 and of the humidity on the fragmentation pattern occur by their effect on the water cluster concentration, indicated by the ratio cps(37)/cps(19), and the different humidity and different CO_2 level of samples can be corrected to a large extent by normalising the measured ncps to a constant ratio cps(37)/cps(19).

Such an effect of water cluster ion concentration on the fragmentation was pointed out by Tani et al. [27] and was explained as follows: the reactions of VOCs of high PA with H_3O^+ via proton transfer reaction are exothermic, and the protonated molecule is internally excited and presumably susceptible to spontaneous or collision-induced dissociation. The reaction with H_3O^+ H_2O, either via proton transfer or via ligand switching, is however less exothermic, and the internal excitation is not sufficient for fragmentation.

The effect of water cluster concentrations on fragmentation pattern may partly explain that this and previous studies reported remarkably different fragmentation patterns for similar values of *E*/*N*. For ethanol, the ratio ncps(29)/ncps(47) of this study resembles the measurements of Blake et al. [34] and of Lagg et al. [33], but it is much lower than the ratio observed by Warneke et al. [35]. For propanol, this study showed a low portion of unfragmentated molecules in agreement with previous measurements [29,35], but the fragment of mass 41 was not mentioned in previous studies. For acetone, this study found no significant fragmentation, similar to Lagg et al. [33], but totally different from Warneke et al. [35]. For isoprene, mass 41 was observed in previous studies but with a lower abundance [30]. It is suspected, however, that not only the different concentrations of water clusters but also the collisions in the intermediate chamber (Fig. 1), located between the sampling orifice of the drift tube and the nosecone of the QMS, have an impact on the observed VOC fragmentation patterns.

3.4. Ageing effect of bag samples

Similar to previous studies [14,36], significant ageing effects of bag samples were observed. Hence, laboratory experiments were conducted to assess the ageing effects and to explore their relation to potential losses of CO_2 from bag samples. Two single mixed expired breath gas samples were collected simultaneously, the first sample in a PTFE bag and the second sample in a FEP bag. The samples were measured four times during the following 3 days at our standard conditions of $E/N = 119$ Td. Between the measurements the samples were stored at room temperature and condensation occurred. Fig. 6a shows the CO_2 concentrations in the bags, calculated from Eq. (2), as a function of the age of the sample. Both types of bags similarly feature a loss of CO_2, the loss being around 80% after 3 days. The ratio of water cluster ions, shown in Fig. 6b, decreases by a factor of three after 77 h, and the decrease is much faster for the FEP bag. The experiments with results presented in Figs. 2 and 4 show that the loss of CO_2 from the bags corresponds to a reduction of the ratio cps(37)/cps(19) of only ~35%. Hence, both types of bags loose not only CO_2 but also water vapour, and the loss is much more rapid for the FEP bag. For the PTFE bag, however, the decrease of the ratio cps(37)/cps(19) within the first 20 h can completely be explained by the loss of CO_2.

The signals of the main breath gas VOCs methanol, ethanol, propanol, acetone and isoprene, were detected on mass 33, 47, 43, 59, and 69 (Fig. 6c and d). During the first 20 h, the only significant change seems to be a decrease of propanol for the FEP bag. This more rapid loss of propanol from the FEP bag is caused by the more rapid loss of water vapour. The loss of water vapour, however, did not affect the signals of methanol, ethanol,

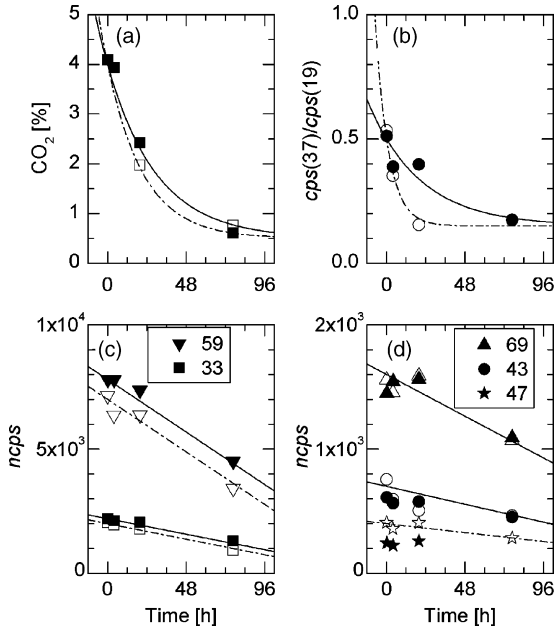

Fig. 6. Ageing effect of breath gas bag samples; displayed are CO_2 concentration (a), ratio of water cluster ions to primary ions (b), and normalised count rates of VOCs (c and d). Solid lines and symbols refer to the PTFE bag, dash-dotted lines and open symbols to the FEP bag. Curves are eye fits to improve lucidity.

acetone and isoprene. Then, after 77 h, all signals had decreased clearly. The decrease also occurred for methanol, acetone and isoprene, where, according to Fig. 4, no significant effect of CO_2 on the measured concentrations could be detected for 119 Td. Fig. 4 also indicates that CO_2 concentrations could substantially contribute to the decrease of the signals for propanol; yet, for ethanol, the decrease of the signal is much weaker than expected, presumably because the ethanol room air concentrations were similar to the concentrations in the bag and the diffusion of ethanol into the bag was low. Hence, for the chosen conditions and the investigated types of bags, the ageing effects are hardly related with the loss of CO_2 but mainly caused by an actual change of VOC concentrations and, for propanol, by the loss of humidity from the bags.

4. Conclusions

The CO_2 concentration in breath gas affects the normalised count rates for strongly fragmenting molecules, and the increase can be, for CO_2 concentrations of 0 and 5%, up to 60%. Hence, VOC-concentrations calculated from PTR-MS signals by the commonly used formula [22] may suffer from large errors. To measure concentrations in breath gas with good accuracy, the PTR-MS should ideally be calibrated with a test gas of appropriate H_2O and CO_2 levels. Moreover, the differences in H_2O and CO_2 levels of individual breath gas samples should be minimised with a well defined sampling method, and the loss of CO_2 from the samples during the storage should be prevented. Such a calibration, however, seems to be difficult, and different levels of humidity and CO_2 in breath gas samples might be inevitable for unusual breathing patterns or for studies which require bag samples. In this case, the comparability of signals can be improved when the effects of CO_2 and humidity are corrected. For that, the signals should be measured as a function of the ratio cps(37)/cps(19); such measurements could be accomplished by adding water to the samples. Then the signals of all samples should be normalised to a constant ratio cps(37)/cps(19).

References

[1] A. Jordan, A. Hansel, R. Holzinger, W. Lindinger, Int. J. Mass Spectrom. (1995) 148.
[2] J. Taucher, A. Hansel, A. Jordan, R. Fall, J.H. Futrell, W. Lindinger, Rapid Commun. Mass Spectrom. 11 (1997) 1230.
[3] T. Karl, P. Prazeller, D. Mayr, A. Jordan, J. Rieder, R. Fall, W. Lindinger, J. Appl. Physiol. 91 (2001) 762.
[4] W. Lindinger, J. Taucher, A. Jordan, A. Hansel, W. Vogel, Alcohol.: Clin. Exp. Res. 21 (1997) 939.
[5] A. Amann, G. Poupart, S. Telser, M. Ledochowski, A. Schmid, S. Mechtcheriakov, Int. J. Mass Spectrom. 239 (2004) 227.
[6] B. Moser, F. Bodrogi, G. Eibl, M. Lechner, J. Rieder, P. Lirk, Respir. Physiol. Neurobiol. 145 (2005) 295.
[7] P. Lirk, F. Bodrogi, J. Rieder, Int. J. Mass Spectrom. 239 (2004) 221.
[8] A. Wehinger, A. Schmid, S. Mechtcheriakov, M. Ledochowski, C. Grabmer, G.A. Gastl, A. Amann, Int. J. Mass Spectrom. 265 (2007) 49.
[9] M. Phillips, Anal. Biochem. 247 (1997) 272.
[10] J.C. Anderson, W.J.E. Lamm, M.P. Hlastala, J. Appl. Physiol. 100 (2006) 880.
[11] J.H. Comroe, Physiology of Respiration, second ed., Year Book Medical Publishers, Chicago, 1965.
[12] K.A. Cope, M.T. Watson, W.M. Foster, S.S. Sehnert, T.H. Risby, J. Appl. Physiol. 96 (2004) 1371.
[13] N.M. Tsoukias, Z. Tannous, A.F. Wilson, S.C. George, J. Appl. Physiol. 85 (1998) 642.
[14] M.M.L. Steeghs, S.M. Cristescu, F.J.M. Harren, Physiol. Meas. 28 (2007) 73.
[15] P. Spanel, D. Smith, J. Phys. Chem. 99 (1995) 15551.
[16] J. de Gouw, C. Warneke, T. Karl, G. Eerdekens, C. van der Veen, R. Fall, Int. J. Mass Spectrom. 223–224 (2003) 365.
[17] C. Warneke, C. van der Veen, S. Luxembourg, J.A. de Gouw, A. Kok, Int. J. Mass Spectrom. 207 (2001) 167.
[18] B.T. Jobson, M.L. Alexander, G.D. Maupin, G.G. Muntean, Int. J. Mass Spectrom. 245 (2005) 78.
[19] L.A. Viehland, S.L. Lin, E.A. Mason, Atom. Data Nucl. Data Tables 60 (1995) 37.
[20] A. Critchley, T.S. Elliott, G. Harrison, C.A. Mayhew, J.M. Thompson, T. Worthington, Int. J. Mass Spectrom. 239 (2004) 235.
[21] W. Lindinger, A. Hansel, A. Jordan, Int. J. Mass Spectrom. Ion Processes 173 (1998) 191.
[22] A. Hansel, A. Jordan, R. Holzinger, P. Prazeller, W. Vogel, W. Lindinger, Int. J. Mass Spectrom. Ion Processes 149/150 (1995) 609.
[23] W. Ma, X. Liu, J. Pawliszyn, Anal. Bioanal. Chem. 385 (2006) 1398.
[24] C. Ammann, A. Brunner, C. Spirig, A. Neftel, Atmos. Chem. Phys. 6 (2006) 4643.
[25] M.M.L. Steeghs, S.M. Cristescu, P. Munnik, P. Zanen, F.J.M. Harren, Physiol. Meas. 28 (2007) 503.
[26] A. Steinbacher, J. Dommen, C. Ammann, C. Spirig, A. Neftel, A.S.H. Prevot, Int. J. Mass Spectrom. 239 (2004) 117.
[27] A. Tani, S. Hayward, A. Hansel, C.N. Hewitt, Int. J. Mass Spectrom. 239 (2004) 161.
[28] J. de Gouw, C. Warneke, Mass Spectrom. Rev. 26 (2007) 223.
[29] C. Warneke, J. Kuczynski, A. Hansel, A. Jordan, W. Vogel, W. Lindinger, Int. J. Mass Spectrom. Ion Processes 154 (1996) 61.
[30] J. Taucher, Ph.D. Thesis, Institute of Ion Physics and Applied Physics, Innsbruck, Austria, 1996.
[31] L. Keck, U. Oeh, C. Hoeschen, Int. J. Mass Spectrom. 264 (2007) 92.
[32] T. Su, W.J. Chesnavich, J. Chem. Phys. 76 (1982) 5183.

[33] A. Lagg, J. Taucher, A. Hansel, W. Lindinger, Int. J. Mass Spectrom. Ion Processes 134 (1994) 55.
[34] R.S. Blake, K.P. Wyche, A.M. Ellis, P.S. Monks, Int. J. Mass Spectrom. 254 (2006) 85.
[35] C. Warneke, J.A. De Gouw, W.C. Kuster, P.D. Goldan, R. Fall, Environ. Sci. Technol. 37 (2003) 2494.
[36] W.A. Groves, E.T. Zellers, Am. Ind. Hyg. Assoc. J. 57 (1996) 257.